



**HAL**  
open science

# Effect of diamagnetic Ca, Sr, Pb, and Ba substitution on the crystal structure and multiferroic properties of the $\text{BiFeO}_3$ perovskite

V. A. Khomchenko, D. A. Kiselev, J. M. Vieira, Li Jian, A. L. Kholkin, A. M. L. Lopes, Y. G. Pogorelov, J. P. Araujo, Mario Maglione

## ► To cite this version:

V. A. Khomchenko, D. A. Kiselev, J. M. Vieira, Li Jian, A. L. Kholkin, et al.. Effect of diamagnetic Ca, Sr, Pb, and Ba substitution on the crystal structure and multiferroic properties of the  $\text{BiFeO}_3$  perovskite. *Journal of Applied Physics*, 2008, 103 (2), 024105 (6 p.). 10.1063/1.2836802 . hal-00280259

**HAL Id: hal-00280259**

**<https://hal.science/hal-00280259>**

Submitted on 5 Mar 2024

**HAL** is a multi-disciplinary open access archive for the deposit and dissemination of scientific research documents, whether they are published or not. The documents may come from teaching and research institutions in France or abroad, or from public or private research centers.

L'archive ouverte pluridisciplinaire **HAL**, est destinée au dépôt et à la diffusion de documents scientifiques de niveau recherche, publiés ou non, émanant des établissements d'enseignement et de recherche français ou étrangers, des laboratoires publics ou privés.

**Effect of diamagnetic Ca, Sr, Pb, and Ba substitution on the crystal structure and multiferroic properties of the BiFeO<sub>3</sub> perovskite**

V. A. Khomchenko, D. A. Kiselev, J. M. Vieira, Li Jian, A. L. Kholkin, A. M. L. Lopes, Y. G. Pogorelov, J. P. Araujo, and M. Maglione

Citation: *Journal of Applied Physics* **103**, 024105 (2008); doi: 10.1063/1.2836802

View online: <http://dx.doi.org/10.1063/1.2836802>

View Table of Contents: <http://scitation.aip.org/content/aip/journal/jap/103/2?ver=pdfcov>

Published by the [AIP Publishing](#)

**Articles you may be interested in**

[Crystal structure and magnetic properties of Bi<sub>0.8</sub>A<sub>0.2</sub>FeO<sub>3</sub> \(A = La, Ca, Sr, Ba\) multiferroics using neutron diffraction and Mossbauer spectroscopy](#)

*AIP Advances* **4**, 087121 (2014); 10.1063/1.4893241

[Influence of diamagnetic Pb doping on the crystal structure and multiferroic properties of the BiFeO<sub>3</sub> perovskite](#)

*J. Appl. Phys.* **105**, 07D918 (2009); 10.1063/1.3079770

[Room temperature multiferroic properties of Eu doped BiFeO<sub>3</sub>](#)

*J. Appl. Phys.* **105**, 07D914 (2009); 10.1063/1.3072087

[Synthesis and multiferroic properties of Bi<sub>0.8</sub>A<sub>0.2</sub>FeO<sub>3</sub> \(A = Ca, Sr, Pb\) ceramics](#)

*Appl. Phys. Lett.* **90**, 242901 (2007); 10.1063/1.2747665

[Multiferroicity in polarized single-phase Bi<sub>0.875</sub>Sm<sub>0.125</sub>FeO<sub>3</sub> ceramics](#)

*J. Appl. Phys.* **100**, 024109 (2006); 10.1063/1.2220642

The new SR865 **2 MHz Lock-In Amplifier ... \$7950**



**SR865 2 MHz DSP Lock-In Amplifier**

**Chart recording**      **FFT displays**      **Trend analysis**

**Features**

- Intuitive front-panel operation
- Touchscreen data display
- Save data & screen shots to USB flash drive
- Embedded web server and iOS app
- Synch multiple SR865s via 10 MHz timebase I/O
- View results on a TV or monitor (HDMI output)

**Specs**

- 1 mHz to 2 MHz
- 2.5 nV/√Hz input noise
- 1 μs to 30 ks time constants
- 1.25 MHz data streaming rate
- Sine out with DC offset
- GPIB, RS-232, Ethernet & USB

**SRS Stanford Research Systems**  
www.thinkSRS.com · Tel: (408)744-9040

# Effect of diamagnetic Ca, Sr, Pb, and Ba substitution on the crystal structure and multiferroic properties of the BiFeO<sub>3</sub> perovskite

V. A. Khomchenko,<sup>1,a)</sup> D. A. Kiselev,<sup>1</sup> J. M. Vieira,<sup>1</sup> Li Jian,<sup>1</sup> A. L. Kholkin,<sup>1</sup>  
A. M. L. Lopes,<sup>2</sup> Y. G. Pogorelov,<sup>2</sup> J. P. Araujo,<sup>2</sup> and M. Maglione<sup>3</sup>

<sup>1</sup>Department of Ceramics and Glass Engineering & CICECO, University of Aveiro, 3810-193 Aveiro, Portugal

<sup>2</sup>IFIMUP/Department of Physics, University of Porto, Rua Campo Alegre 687, 4169-007 Porto, Portugal

<sup>3</sup>Institut de Chimie de la Matière Condensée de Bordeaux, CNRS-Université Bordeaux I, 87, Avenue du Dr. A. Schweitzer, 33608 Pessac, France

(Received 8 August 2007; accepted 30 November 2007; published online 28 January 2008)

In this work, we studied the effect of heterovalent Ca, Sr, Pb, and Ba substitution on the crystal structure, dielectric, local ferroelectric, and magnetic properties of the BiFeO<sub>3</sub> multiferroic perovskite. Ceramic solid solutions with the general formula Bi<sub>0.7</sub>A<sub>0.3</sub>FeO<sub>3</sub> (A is a doping element) were prepared and characterized by x-ray diffraction, dielectric, piezoresponse force microscopy (PFM), and magnetic measurements. It is shown that the crystal structure of the compounds is described within the space group *R3c*, permitting the spontaneous polarization, whose existence was confirmed by the PFM data. Magnetic properties of the solid solutions are determined by the ionic radius of the substituting element. Experimental results suggest that the increase in the radius of the A-site ion leads to the effective suppression of the spiral spin structure of BiFeO<sub>3</sub>, resulting in the appearance of net magnetization. © 2008 American Institute of Physics. [DOI: [10.1063/1.2836802](https://doi.org/10.1063/1.2836802)]

## I. INTRODUCTION

In the last few years there has been a revival of interest in the study of multiferroics,<sup>1,2</sup> which have great potential for the creation of magnetoelectric and magneto-optical devices. Indeed, strong coupling between ferroelectric and magnetic order parameters in these materials, for which external magnetic field induces a change of the ferroelectric characteristics and electric field induces a change of the magnetization, would allow developing a whole range of technological innovations, including memory media with ferroelectric writing and magnetic reading. However, known single-phase magnetic ferroelectrics usually have low magnetic ordering temperatures,<sup>3-7</sup> thus constricting the possibilities for their application. From this point of view, the most interesting results are expected for the BiFeO<sub>3</sub>-based perovskite materials. Indeed, BiFeO<sub>3</sub> possesses a magnetic ordering and a ferroelectric polarization at room temperature (the Néel temperature is about 640 K, and the ferroelectric Curie temperature is about 1100 K). Though this property is very promising in terms of practical applications, the magnetic ordering is of antiferromagnetic type, having a spatially modulated spin structure,<sup>8</sup> which does not allow net magnetization and also inhibits the observation of the linear magnetoelectric effect.<sup>9</sup> It has been suggested that this spin configuration can be suppressed with the application of a high magnetic field,<sup>9-11</sup> an epitaxial constraint,<sup>12</sup> or a doping.<sup>13-20</sup>

The enhancement of magnetization has been reported for the Bi<sub>1-x</sub>A<sub>x</sub>FeO<sub>3</sub> (A=lanthanide or Ba)<sup>13-17</sup> and BiFeO<sub>3</sub>-LnFeO<sub>3</sub>-ATiO<sub>3</sub> (Ln=lanthanide; A=Pb, Ba)<sup>18-20</sup> solid solutions. The highest values of the spontaneous magnetization have been observed for the rare-earth doped samples, in

which strong contribution from magnetic moments of the rare-earth ions to the net magnetization takes place. In case of diamagnetic A-site doping of BiFeO<sub>3</sub>, the only possible reason for the appearance of spontaneous magnetization is through weak ferromagnetism,<sup>21,22</sup> allowed by the symmetry of the crystal structure of BiFeO<sub>3</sub>.<sup>23,24</sup> In these compounds, the value of the net magnetization depends strongly on the kind of substituting element. For instance, the spontaneous magnetization of the Ba-doped samples is at least an order of magnitude greater than that observed for the La-doped solid solutions at the same doping concentration.<sup>13,17</sup>

In order to unveil the main regularities of changes of the magnetic properties of the BiFeO<sub>3</sub>-based multiferroics under diamagnetic A-site doping and to understand the A<sup>2+</sup> doping effect on the dielectric and ferroelectric properties of BiFeO<sub>3</sub>, we have performed synthesis and structural, magnetic, dielectric, and local ferroelectric investigation of the Bi<sub>0.7</sub>A<sub>0.3</sub>FeO<sub>3</sub> (A=Ca, Sr, Pb, Ba) ceramics (preliminary research has shown that the solid solubility level is about 30% for Pb and Ba substitution in BiFeO<sub>3</sub>).<sup>25</sup> The existence of ferroelectric polarization in all samples at room temperature has been confirmed by piezoresponse force microscopy. Strong correlation between the ionic radius of the substituting element and the value of the spontaneous magnetization of the sintered ceramics has been found.

## II. EXPERIMENT

Bi<sub>0.7</sub>A<sub>0.3</sub>FeO<sub>3</sub> (A=Ca, Sr, Pb, Ba) solid solutions were prepared by a rapid two-stage solid-state reaction method using high-purity Bi<sub>2</sub>O<sub>3</sub>, Fe<sub>2</sub>O<sub>3</sub>, CaCO<sub>3</sub>, SrCO<sub>3</sub>, BaCO<sub>3</sub>, and PbO reagents. The compacted mixtures of reagents taken in desired cation ratios were annealed at 800 °C (Pb) or 850 °C (Ca, Sr, Ba) for 30 min in air to obtain single-phase

<sup>a)</sup>Electronic mail: khomchenko@cv.ua.pt.

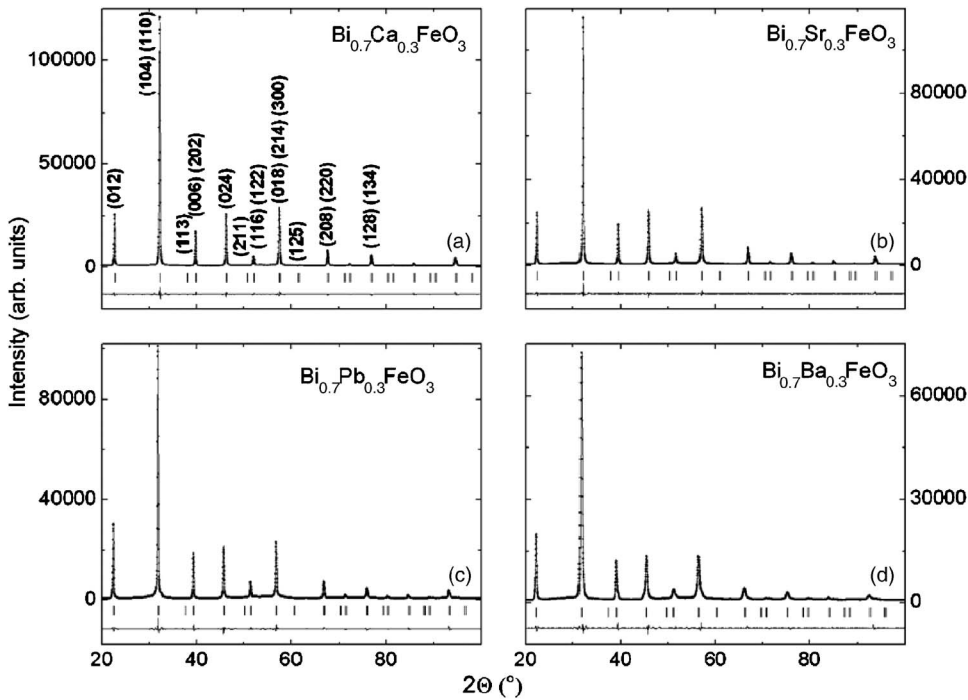


FIG. 1. Rietveld refinement of the XRD pattern for the  $\text{Bi}_{0.7}\text{A}_{0.3}\text{FeO}_3$  samples at room temperature (space group  $R3c$ ). The difference between observed (solid circles) and calculated (solid line) spectra is plotted at the bottom. Bragg reflections are indicated by ticks.

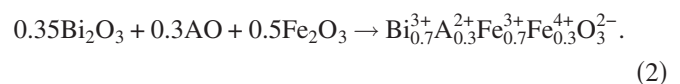
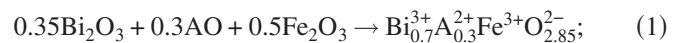
perovskite. Final heat-treatment was performed in the temperature range from 840 °C (Pb) to 990 °C (Sr) for 10 min to produce relatively dense ceramics. The maximal synthesis temperatures were close to the melting points of the solid solutions. All the compounds were quenched by removing the sample from the furnace immediately after sintering. The crystal structure of the samples was determined with x-ray diffraction (XRD) data. XRD patterns were collected at room temperature using a Rigaku D/MAX-B diffractometer with  $\text{Cu } K\alpha$  radiation. The data were analyzed by the Rietveld method using the FullProf program. The dielectric characteristics of the samples were measured in the temperature range from 80 to 400 K using a HP4194A impedance analyzer in a frequency range from 1 kHz to 10 MHz. The ferroelectric hysteresis loops were obtained with the conventional Sawyer–Tower method using an oscilloscope LT322 (LeCroy). Measurements of the field dependencies of the magnetization were performed with a superconducting quantum interference device magnetometer (MPMS-5, Quantum Design). Local ferroelectric properties of the samples were investigated with piezoresponse force microscopy (PFM). PFM measurements were performed with a commercial setup (Multimode, NanoScope IIIA, Veeco) equipped with a lock-in amplifier (SR-830A, Stanford Research) and a function generator (FG-120, Yokogawa). A commercial tip-cantilever system NSG11 (NT-MDT) with the spring constant of 10 N/m and TiN-coated tip with apex radius less than 10 nm were used. Domain visualization was performed under an applied ac voltage with the amplitude  $V_{ac}=2.5$  V and frequency  $f=50$  kHz. Local poling was done by applying a dc bias of  $\pm 10$  V between the tip and counter electrode followed by a consequent PFM imaging.

### III. RESULTS AND DISCUSSION

$\text{BiFeO}_3$  is known to have a rhombohedrally distorted perovskite structure described by the space group  $R3c$ .<sup>26</sup> The

rhombohedral cell is very close to the cubic one (angle  $\alpha$  in the rhombohedral cell is about 89.4°). In this structure, the cations are displaced from their centrosymmetric positions along the pseudocubic  $[111]_C$  axis (or corresponding  $[001]_H$  axis in the hexagonal basis), and the oxygen octahedra rotate with alternating sense around this direction. The cation displacement leads to the appearance of spontaneous polarization oriented along  $[001]_H$ . In accordance with the structural data obtained for the parent compound, Rietveld refinement of the x-ray powder diffraction patterns of the doped samples was performed using the same space group, and the structural model allowed us to reproduce adequately all the observed reflections. Good agreement between the observed and calculated XRD patterns obtained for the  $\text{Bi}_{0.7}\text{A}_{0.3}\text{FeO}_3$  samples is shown in Fig. 1. The structural parameters of the compounds are presented in Table I. Unlike a number of publications on lanthanide-doped samples<sup>13–15</sup> (reporting substitution-induced structural phase transitions to orthorhombic or even triclinic phase), no splitting or extra reflections indicative of the necessity to reduce the lattice symmetry of synthesized ceramics were detected (Fig. 1). The unit cell volume of the studied samples varies in accordance with the ionic radius values<sup>27</sup> of the substituting elements, as demonstrated in Table I.

The heterovalent  $\text{Bi}^{3+}$  to  $\text{A}^{2+}$  substitution in  $\text{Bi}_{0.7}\text{A}_{0.3}\text{FeO}_3$  requires the appearance of oxygen vacancies or/and  $\text{Fe}^{4+}$  ions in the host lattice, in accordance with the following defect chemistry models:



It is important to investigate the influence of the  $\text{A}^{2+}$  doping on the dielectric properties of  $\text{Bi}_{0.7}\text{A}_{0.3}\text{FeO}_3$  com-

TABLE I. Structural parameters for the  $\text{Bi}_{0.7}\text{A}_{0.3}\text{FeO}_3$  compounds obtained by Rietveld refinement of the XRD patterns at room temperature. Space group  $R3c$ .

Sample	Cell (Å)	Atom	Position	$x$	$y$	$z$	$R$ factors (%)
$\text{Bi}_{0.7}\text{Ca}_{0.3}\text{FeO}_3$	$a=5.5395(1)$	Bi/Ca	$6a$	0	0	0.2528(8)	$R_p=3.02$
	$c=13.5674(1)$	Fe	$6a$	0	0	0	$R_{wp}=4.05$
	$V=360.55(4)$	O	$18b$	0.8091(26)	0.6475(14)	0.4541(8)	$R_B=1.13$
							$\chi^2=3.26$
$\text{Bi}_{0.7}\text{Sr}_{0.3}\text{FeO}_3$	$a=5.5870(1)$	Bi/Sr	$6a$	0	0	0.2534(8)	$R_p=3.10$
	$c=13.6845(1)$	Fe	$6a$	0	0	0	$R_{wp}=4.21$
	$V=369.93(5)$	O	$18b$	0.8218(23)	0.6496(17)	0.4537(10)	$R_B=1.16$
							$\chi^2=3.61$
$\text{Bi}_{0.7}\text{Pb}_{0.3}\text{FeO}_3$	$a=5.6004(1)$	Bi/Pb	$6a$	0	0	0.2529(9)	$R_p=3.22$
	$c=13.7291(1)$	Fe	$6a$	0	0	0	$R_{wp}=4.43$
	$V=372.92(6)$	O	$18b$	0.8158(28)	0.6452(18)	0.4546(11)	$R_B=1.20$
							$\chi^2=3.72$
$\text{Bi}_{0.7}\text{Ba}_{0.3}\text{FeO}_3$	$a=5.6368(1)$	Bi/Ba	$6a$	0	0	0.2542(9)	$R_p=3.16$
	$c=13.8392(1)$	Fe	$6a$	0	0	0	$R_{wp}=4.32$
	$V=380.80(7)$	O	$18b$	0.8204(26)	0.6452(17)	0.4590(10)	$R_B=1.18$
							$\chi^2=3.65$

pounds because the heterovalent substitution-induced defects may cause high leakage current, which apparently decreases the dielectric breakdown field and thus prevents the poling of the samples. Temperature dependencies of the dielectric constant and dielectric loss for the  $\text{Bi}_{0.7}\text{A}_{0.3}\text{FeO}_3$  compounds at different frequencies are shown in Fig. 2. Strong increase of the dielectric characteristics is observed with increasing temperature or decreasing frequency. The behavior can be qualitatively explained in the following way:<sup>15,28</sup> the defects-related dipoles are able to follow the alternating field at low frequencies, providing high values of

$\epsilon'$ , but begin to lag behind the field with increasing frequency, giving  $\epsilon' \approx 70$  and  $\tan \delta \approx 0.02$  (at room temperature), which is comparable with the values observed in pure  $\text{BiFeO}_3$  and isovalent substituted  $\text{Bi}_{1-x}\text{RE}_x\text{FeO}_3$  ceramics.<sup>14,15</sup> The increase of the dielectric permittivity and loss factor with increasing temperature is then related to thermally induced enhancement of the hopping conduction. High values of dielectric loss observed in  $\text{Bi}_{0.7}\text{A}_{0.3}\text{FeO}_3$  samples above 250–300 K (Fig. 2) suggest that the materials can be considered promising for practical applications mainly below room temperature.

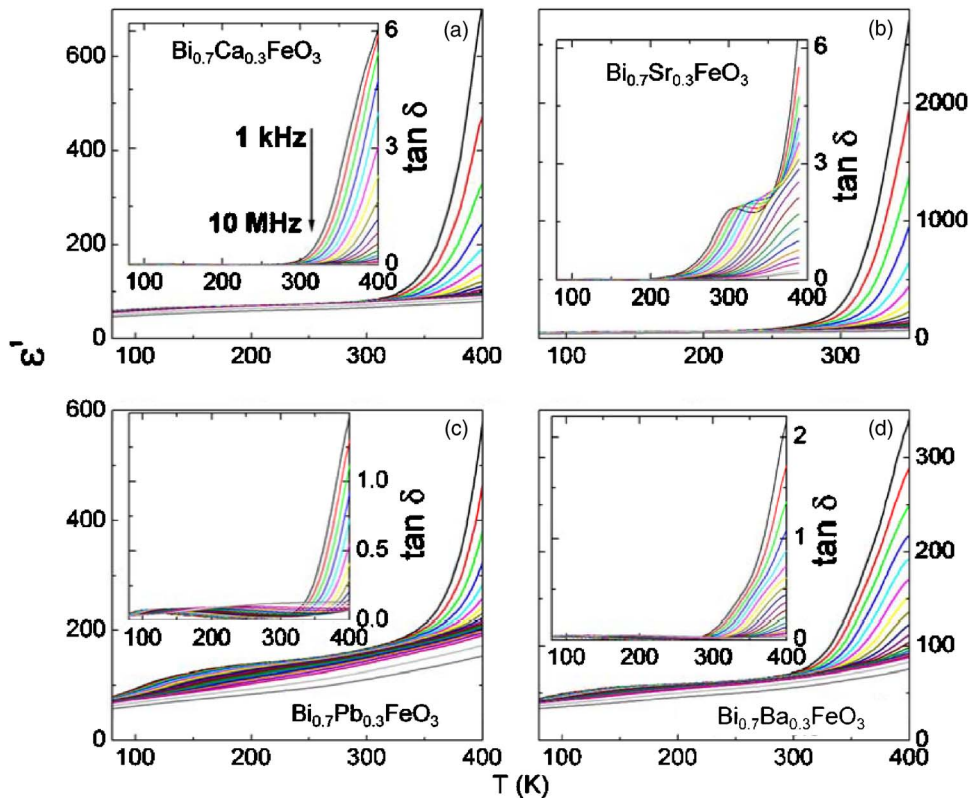


FIG. 2. (Color online) Temperature dependencies of the dielectric constant and dielectric loss (in insets) for the  $\text{Bi}_{0.7}\text{A}_{0.3}\text{FeO}_3$  samples at different frequencies.

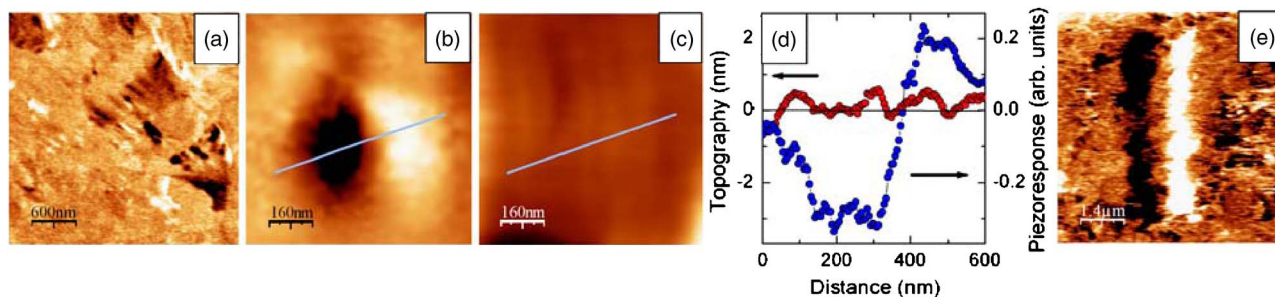


FIG. 3. (Color online) Piezoresponse force microscopy measurements of  $\text{Bi}_{0.7}\text{Ca}_{0.3}\text{FeO}_3$  ceramics: (a), (b) PFM images demonstrating ferroelectric domains; (c) topography; (d) cross section of the PFM image showing absence of correlation between the topography and piezoresponse; (e) electric-field-induced PFM contrast ( $V=10 \pm V$ ).

Measurements of the ferroelectric hysteresis loops by the conventional Sawyer–Tower method have been undertaken at room temperature to estimate the spontaneous polarization values of the samples under study. It has been found that the ferroelectric hysteresis loops have rounded corners, indicating significant conductive losses. Very similar results have been previously obtained for other Bi-based solid solutions and composites, such as  $\text{Bi}_{1-x}\text{Ba}_x\text{FeO}_3$ ,<sup>17</sup>  $\text{Bi}_2\text{FeCrO}_6$ ,<sup>29</sup>  $\text{Bi}_2\text{NiMnO}_6$ ,<sup>30</sup>  $\text{BiFeO}_3\text{–LnFeO}_3\text{–ATiO}_3$  (Ln=lanthanide; A=Pb, Ba),<sup>18,19</sup> and  $\text{Bi}_2\text{Fe}_4\text{O}_9\text{–BaO}$ .<sup>31</sup> No saturation of the polarization has been observed up to the dielectric breakdown fields ( $\sim 100$  kV/cm), making evaluation of the spontaneous polarization impossible. Thus, no definite conclusion proving the existence of spontaneous polarization in the  $\text{Bi}_{0.7}\text{A}_{0.3}\text{FeO}_3$  samples at room temperature could be made on the basis of the polarization vs electric field measurements.

The piezoresponse force microscopy technique has been used for the visualization of domain structure in the  $\text{Bi}_{0.7}\text{A}_{0.3}\text{FeO}_3$  compounds to ascertain the existence of spontaneous polarization (see, e.g., Ref. 32 and references therein). The PFM method is based on the detection of thickness oscillations of ferroelectric materials under ac voltage applied between the conductive scanning probe microscope tip and the bottom electrode. The amplitude of the vibration signal  $A$  provides information on the magnitude of the effective piezoelectric coefficient, while the phase signal  $\varphi$  determines the polarization direction. Domains with oppositely oriented polarization are distinguished by different contrast (proportional to  $A \cos \varphi$ ). In our experiments, the bright and dark contrasts correspond to domains with polarization vector directed to the free surface of the ceramics and to the bulk, respectively. The piezoelectric contrast was revealed on the surface of all investigated samples. An example of these measurements for  $\text{Bi}_{0.7}\text{Ca}_{0.3}\text{FeO}_3$  is shown in Fig. 3. It is seen that the areas with intermediate contrast corresponding to regions with defect structure suppressing any PFM signal coexist with areas exhibiting clear piezoresponse corresponding to antiparallel domains [Fig. 3(a)]. In spite of the appreciable roughness of the surfaces, masking the contribution of the piezoelectric deformation to the PFM contrast, only a weak correlation has been found between the topography and piezoresponse [Figs. 3(b)–3(d)], pointing to the weak contribution of the electrostatic signal.<sup>32</sup> The piezoelectric contrast appears also after scanning with a dc voltage applied to the

tip [Fig. 3(e)], giving clear proof that the spontaneous polarization can be switched upon the application of electric field. In comparing current results with those obtained on  $\text{Bi}_{0.8}\text{A}_{0.2}\text{FeO}_3$  (A=Ca, Sr, Pb) ceramic samples,<sup>33</sup> a notable reduction of the amplitude of the measured vibrations is observed, indicating decrease of the effective longitudinal piezoelectric coefficient and, thus, polarization due to the presence of A-site dopants. This means that the regular polar displacement caused by stereochemical activity of the  $6s^2$  lone pair on  $\text{Bi}^{3+}$  ions, giving rise to ferroelectricity in  $\text{BiFeO}_3$ -based solids,<sup>34</sup> is suppressed by the A-site doping of  $\text{BiFeO}_3$ . Regular domain structure has been recently reported on single-crystalline grains of  $\text{BiFeO}_3$  ceramics.<sup>35</sup> These ferroelectric domains are considerably larger than those observed in our experiments. This may be explained by the difference in sintering conditions: i.e., the increased duration of the thermal treatment at the temperature far below melting point being used to prepare the  $\text{BiFeO}_3$  sample<sup>35</sup> has apparently ensured stress suppression and higher quality of the grains. However, we did not succeed in obtaining single-phase  $\text{Bi}_{0.7}\text{A}_{0.3}\text{FeO}_3$  perovskites using a similar method.

Investigation of magnetic properties of the  $\text{Bi}_{0.7}\text{A}_{0.3}\text{FeO}_3$  compounds revealed a distinct correlation between the ionic radius of the substituting element and the spontaneous magnetization. Magnetization of the samples as a function of applied magnetic field is shown in Fig. 4. The  $M(H)$  dependency obtained for Ca-doped compound [with the smallest unit cell volume (Table I)] reproduces a linear coupling characteristic of pure  $\text{BiFeO}_3$ <sup>36,37</sup> without any spontaneous magnetization, thus indicating the antiferromagnetic nature of the sample. Weak spontaneous magnetization of 0.08 emu/g appears in Sr-doped compound. Further increase of magnetization value is observed for  $\text{Bi}_{0.7}\text{Pb}_{0.3}\text{FeO}_3$  solid solution. Maximal spontaneous magnetization of 1.2 emu/g ( $\sim 0.06 \mu_B$  per formula unit) was obtained for the sample doped with  $\text{Ba}^{2+}$ , possessing the biggest ionic radius value.<sup>27</sup> All the nonantiferromagnetic samples had almost the same coercive fields of 3.2 kOe.

Magnetic properties of the diamagnetically doped  $\text{Bi}_{1-x}\text{A}_x\text{FeO}_3$  compounds are entirely determined by the magnetically active iron sublattice. Because the possible superexchange interactions  $\text{Fe}^{3+}\text{–O–Fe}^{3+}$  or  $\text{Fe}^{3+}\text{–O–Fe}^{4+}$  (if the heterovalent substitution in these compounds is realized through the  $\text{Fe}^{4+}$  ion's appearance) are antiferromagnetic, the only intrinsic reason for the existence of spontaneous mag-

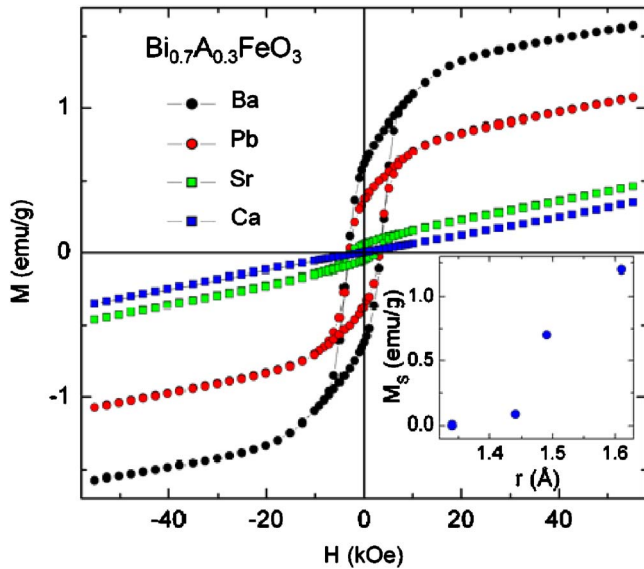


FIG. 4. (Color online) Field dependences of magnetization for the  $\text{Bi}_{0.7}\text{A}_{0.3}\text{FeO}_3$  ceramics at room temperature. Inset shows spontaneous magnetization of the samples as a function of the ionic radius of the dopant.

netization in the  $\text{Bi}_{0.7}\text{A}_{0.3}\text{FeO}_3$  is a canting of the antiferromagnetic sublattices (weak ferromagnetism),<sup>21,22</sup> permitted by the  $R3c$  symmetry, if the magnetic moments are oriented perpendicular to the  $[001]_H$  axis.<sup>24</sup> The commonalities of the spontaneous magnetization appearance suggest that the transition from the spiral spin structure to the homogeneous magnetic state in  $\text{BiFeO}_3$ -based compounds can be induced by the application of high magnetic fields,<sup>9–11</sup> epitaxial constraint,<sup>12</sup> or doping.<sup>13–20</sup> For all the cases, the theoretical description of the transition has been proposed based on Landau–Ginzburg formalism for the free energy.<sup>9–12,20</sup> However, the presented thermodynamic model seems to be unable to describe all the existing experimental data. For instance, this model, which takes into account a magnetoelectric coupling, suggests that doping-induced destruction of the spiral spin structure results in a significant enhancement of the spontaneous polarization of the sample.<sup>20</sup> The opposite is experimentally observed: dilution of Bi sublattice in  $\text{Bi}_{1-x}\text{Ln}_x\text{FeO}_3$  solids naturally decreases both the ferroelectric Curie temperature and the spontaneous polarization value, the magnetization being increased.<sup>14,38</sup> A dramatic increase in the electric-field-induced polarization of  $\text{BiFeO}_3$ – $\text{PbTiO}_3$ -based solid solutions ( $P_r \approx 30 \mu\text{C}/\text{cm}^2$ ) in comparison with pure  $\text{BiFeO}_3$  crystal ( $P_r$  is an order of magnitude lower) was probably the experimental basis of the model.<sup>20</sup> In reality, the spontaneous polarization of single-crystal  $\text{BiFeO}_3$  is close to the theoretically predicted value of  $90 \mu\text{C}/\text{cm}^2$  (Ref. 39) and seems to be mainly determined by the quality of the material.<sup>35,40</sup> Similar serious contradictions exist in the theoretical description adapted to the case of epitaxial films of  $\text{BiFeO}_3$ ,<sup>12</sup> whose polarization and magnetization are not very sensitive to strain,<sup>35,41–44</sup> while the theoretical model suggest their strong dependence. Thus, the proposed theoretical approach should be reconsidered.

The introduction of A-site impurities results in the variation of the anisotropy constant and thus provokes the transition from a spatially modulated spin structure to a homoge-

neously canted one. Such a canting arises from the Dzyaloshinskii–Moriya interaction, and its magnitude is determined by the strength of the spin-orbital coupling.<sup>21,22</sup> In  $\text{BiFeO}_3$ , as in the common case of the transition metal-based compounds, the interaction energy of the orbital moment of 3d electrons with an external magnetic field,  $\Delta_H$ , is significantly less than the value of the crystal-field-induced level splitting,  $\Delta_{\text{cryst}}$ . This means that magnetic field is only a weak perturbation in comparison with the electric field of the crystal lattice and is thus unable to influence the orientation of the orbital moment, so total magnetic moment contains a spin moment contribution only. However, spin-orbit interaction with energy  $\Delta_{LS}$  ( $\Delta_H < \Delta_{LS} < \Delta_{\text{cryst}}$ ) prevents the complete “freezing” of orbital moment and induces minor magnetic moment [ $\sim(\Delta_{LS}/\Delta_{\text{cryst}})\mu_B$ ] related to the electron orbital motion. This moment determines the orientation of the spin moment in the crystal lattice, thus causing magnetic anisotropy and shifting the  $g$  factor from the value, predicted for spin-only moment ( $g=2$ ). All the effects are enhanced with increasing the ratio  $\Delta_{LS}/\Delta_{\text{cryst}}$ . Electron magnetic resonance measurements have shown a coupling between the increase of the  $g$  value and the appearance of spontaneous magnetization in  $\text{BiFeO}_3$  with La doping.<sup>45</sup> Accordingly, the observed correlation between the ionic radius of the substituting element and the magnetic properties of  $\text{Bi}_{0.7}\text{A}_{0.3}\text{FeO}_3$  [i.e., spontaneous magnetization appears in compounds doped by bigger ions (see inset to Fig. 4)] can reflect the ability of the dopants to perturb the ligand field more effectively, thus inducing the transition from a spiral spin structure to a weak ferromagnetic state.

#### IV. CONCLUSIONS

Investigation of the crystal structure, dielectric, local ferroelectric, and magnetic properties of  $\text{Bi}_{0.7}\text{A}_{0.3}\text{FeO}_3$  ( $\text{A} = \text{Ca}, \text{Sr}, \text{Pb}, \text{Ba}$ ) perovskites was carried out. X-ray diffraction measurements showed that the samples are single-phase perovskites and their crystal structure is described by the noncentrosymmetric  $R3c$  space group. Piezoresponse force microscopy data confirmed the existence of the spontaneous polarization in these compounds at room temperature. Magnetization measurements showed that the magnetic state of the samples is determined by the ionic radius of the substituting elements, and dopants with the biggest ionic radius effectively suppress the spiral spin structure of  $\text{BiFeO}_3$ . This paves the way for the promising development of  $\text{BiFeO}_3$ -based multiferroic materials possessing spontaneous magnetization and ferroelectric polarization at room temperature. The magnetic properties were discussed in terms of doping-induced changes in the magnetic anisotropy.

#### ACKNOWLEDGMENTS

V. A. Khomchenko is grateful to the Foundation for Science and Technology of Portugal (FCT) for the financial support (grant SFRH/BPD/26163/2005). The work was done within EC-funded project “Multiceral” (NMP3-CT-2006-032616) and Network of Excellence “FAME” (NMP3-CT-2004-500159).

- <sup>1</sup>S.-W. Cheong and M. Mostovoy, *Nat. Mater.* **6**, 13 (2007).
- <sup>2</sup>W. Eerenstein, N. D. Mathur, and J. F. Scott, *Nature (London)* **442**, 759 (2006).
- <sup>3</sup>M. Fiebig, D. Fröhlich, K. Kohn, St. Leute, Th. Lottermoser, V. V. Pavlov, and R. V. Pisarev, *Phys. Rev. Lett.* **84**, 5620 (2000).
- <sup>4</sup>A. V. Kimel, R. V. Pisarev, F. Bentivegna, and Th. Rasing, *Phys. Rev. B* **64**, 201103 (2001).
- <sup>5</sup>T. Katsufuji, M. Masaki, A. Machida, M. Moritomo, K. Kato, E. Nishibori, M. Takata, M. Sakata, K. Ohoyama, K. Kitazawa, and H. Takagi, *Phys. Rev. B* **66**, 134434 (2002).
- <sup>6</sup>T. Kimura, S. Kawamoto, I. Yamada, M. Azuma, M. Takano, and Y. Tokura, *Phys. Rev. B* **67**, 180401(R) (2003).
- <sup>7</sup>T. Goto, T. Kimura, G. Lawes, A. P. Ramirez, and Y. Tokura, *Phys. Rev. Lett.* **92**, 257201 (2004).
- <sup>8</sup>I. Sosnowska, T. Peterlin-Neumaier, and E. Steichele, *J. Phys. C* **15**, 4835 (1982).
- <sup>9</sup>Yu. F. Popov, A. K. Zvezdin, G. P. Vorob'ev, A. M. Kadomtseva, V. A. Murashev, and D. N. Rakov, *JETP Lett.* **57**, 69 (1993).
- <sup>10</sup>A. M. Kadomtseva, A. K. Zvezdin, Yu. F. Popov, A. P. Pyatakov, and G. P. Vorob'ev, *JETP Lett.* **79**, 571 (2004).
- <sup>11</sup>B. Ruetter, S. Zvyagin, A. P. Pyatakov, A. Bush, J. F. Li, V. I. Belotelov, A. K. Zvezdin, and D. Viehland, *Phys. Rev. B* **69**, 064114 (2004).
- <sup>12</sup>F. Bai, J. Wang, M. Wutting, J. F. Li, N. Wang, A. P. Pyatakov, A. K. Zvezdin, L. E. Cross, and D. Viehland, *Appl. Phys. Lett.* **86**, 032511 (2005).
- <sup>13</sup>S.-T. Zhang, Y. Zhang, M.-H. Lu, C.-L. Du, Y.-F. Chen, Z.-G. Liu, Y.-Y. Zhu, N.-B. Ming, and X. Q. Pan, *Appl. Phys. Lett.* **88**, 162901 (2006).
- <sup>14</sup>G. L. Yuan, S. W. Or, J. M. Liu, and Z. G. Liu, *Appl. Phys. Lett.* **89**, 052905 (2006).
- <sup>15</sup>G. L. Yuan and S. W. Or, *J. Appl. Phys.* **100**, 024109 (2006).
- <sup>16</sup>V. R. Palkar, D. C. Kundaliya, S. K. Malik, and S. Bhattacharya, *Phys. Rev. B* **69**, 212102 (2004).
- <sup>17</sup>D. H. Wang, W. C. Goh, M. Ning, and C. K. Ong, *Appl. Phys. Lett.* **88**, 212907 (2006).
- <sup>18</sup>J. S. Kim, C. I. Cheon, Y. N. Choi, and P. W. Jang, *J. Appl. Phys.* **93**, 9263 (2003).
- <sup>19</sup>J. S. Kim, C. I. Cheon, C. H. Lee, and P. W. Jang, *J. Appl. Phys.* **96**, 468 (2004).
- <sup>20</sup>N. Wang, J. Cheng, A. Pyatakov, A. K. Zvezdin, J. F. Li, L. E. Cross, and D. Viehland, *Phys. Rev. B* **72**, 104434 (2005).
- <sup>21</sup>I. E. Dzyaloshinskii, *Sov. Phys. JETP* **5**, 1259 (1957).
- <sup>22</sup>T. Moriya, *Phys. Rev.* **120**, 91 (1960).
- <sup>23</sup>I. Sosnowska, M. Loewenhaupt, W. I. F. David, and R. M. Ibberson, *Mater. Sci. Forum* **133–136**, 683 (1993).
- <sup>24</sup>C. Ederer and N. A. Spaldin, *Phys. Rev. B* **71**, 060401(R) (2005).
- <sup>25</sup>V. A. Khomchenko, D. A. Kiselev, J. M. Vieira, A. M. L. Lopes, Y. G. Pogorelov, J. P. Araujo, M. Maglione, and A. L. Kholkin (unpublished).
- <sup>26</sup>C. Michel, J.-M. Moreau, G. D. Achenbach, R. Gerson, and W. J. James, *Solid State Commun.* **7**, 701 (1969).
- <sup>27</sup>R. D. Shannon, *Acta Crystallogr., Sect. A: Cryst. Phys., Diffraction, Theor. Gen. Crystallogr.* **32**, 751 (1976).
- <sup>28</sup>A. Dutta and T. P. Sinha, *J. Phys. Chem. Solids* **67**, 1484 (2006).
- <sup>29</sup>R. Nechache, C. Harnagea, A. Pignolet, F. Normandin, T. Veres, L.-P. Carignan, and D. Ménard, *Appl. Phys. Lett.* **89**, 102902 (2006).
- <sup>30</sup>M. Sakai, A. Masuno, D. Kan, M. Hashisaka, K. Takata, M. Azuma, M. Takano, and Y. Shimakawa, *Appl. Phys. Lett.* **90**, 072903 (2007).
- <sup>31</sup>D. H. Wang and C. K. Ong, *J. Appl. Phys.* **100**, 044111 (2006).
- <sup>32</sup>A. L. Kholkin, S. V. Kalinin, A. Roelofs, and A. Gruverman, in *Scanning Probe Microscopy: Electrical and Electromechanical Phenomena at the Nanoscale*, edited by S. Kalinin and A. Gruverman (Springer, New York, 2006), Vol. 1, pp. 173–214.
- <sup>33</sup>V. A. Khomchenko, D. A. Kiselev, J. M. Vieira, A. L. Kholkin, M. A. Sá, and Y. G. Pogorelov *Appl. Phys. Lett.* **90**, 242901 (2007).
- <sup>34</sup>R. Seshadri and N. A. Hill, *Chem. Mater.* **13**, 2892 (2001).
- <sup>35</sup>V. V. Shvartsman, W. Kleemann, R. Haumont, and J. Kreisel, *Appl. Phys. Lett.* **90**, 172115 (2007).
- <sup>36</sup>Q.-H. Jiang, C.-W. Nan, and Z.-J. Shen, *J. Am. Ceram. Soc.* **89**, 2123 (2006).
- <sup>37</sup>F. Chen, Q. F. Zhang, J. H. Li, Y. J. Qi, C. J. Lu, X. B. Chen, X. M. Ren, and Y. Zhao, *Appl. Phys. Lett.* **89**, 092910 (2006).
- <sup>38</sup>H. Uchida, R. Ueno, H. Funakubo, and S. Koda, *J. Appl. Phys.* **100**, 014106 (2006).
- <sup>39</sup>J. B. Neaton, C. Ederer, U. V. Waghmare, N. A. Spaldin, and K. M. Rabe, *Phys. Rev. B* **71**, 014113 (2005).
- <sup>40</sup>D. Lebeugle, D. Colson, A. Forget, M. Viret, P. Bonville, J. F. Marucco, and S. Fusil, *Phys. Rev. B* **76**, 024116 (2007).
- <sup>41</sup>C. Ederer and N. A. Spaldin, *Phys. Rev. B* **71**, 224103 (2005).
- <sup>42</sup>J. Wang, J. B. Neaton, H. Zheng, V. Nagarajan, S. B. Ogale, B. Liu, D. Viehland, V. Vaithyanathan, D. G. Schlom, U. V. Waghmare, N. A. Spaldin, K. M. Rabe, M. Wuttig, and R. Ramesh, *Science* **299**, 1719 (2003).
- <sup>43</sup>W. Eerenstein, F. D. Morrison, J. Dho, M. G. Blamire, J. F. Scott, and N. D. Mathur, *Science* **307**, 1203a (2005).
- <sup>44</sup>H. Béa, M. Bibes, S. Fusil, K. Bouzehouane, E. Jacquet, K. Rode, P. Bencok, and A. Barthélémy, *Phys. Rev. B* **74**, 020101(R) (2006).
- <sup>45</sup>S. R. Das, R. N. P. Choudhary, P. Bhattacharya, R. S. Katiyar, P. Dutta, A. Manivannan, and M. S. Seehra, *J. Appl. Phys.* **101**, 034104 (2007).